THE FLORIDA STATE UNIVERSITY

COLLEGE OF ARTS AND SCIENCES

INVESTIGATION OF THE RELATIONSHIP BETWEEN THE YUCATAN CHANNEL TRANSPORT AND THE LOOP CURRENT AREA IN A MULTI-DECADAL NUMERICAL SIMULATION

By

ROBERT NEDBOR-GROSS

A Thesis submitted to the
Department of Earth, Ocean and Atmospheric Science
in partial fulfillment of the
requirements for the degree of
Master of Science

Degree Awarded:
Fall Semester, 2013

Robert Nedbor-Gross defended this thesis on August 30, 2013.
The members of the supervisory committee were:

Mark A. Bourassa
Professor Directing Thesis

Dmitry S. Dukhovskoy
Committee Member

Steven L. Morey
Committee Member

Eric P. Chassignet
Committee Member

Philip Sura
Committee Member

The Graduate School has verified and approved the above-named committee members, and certifies that the thesis has been approved in accordance with university requirements.

This thesis is dedicated to my family and friends.

TABLE OF CONTENTS

LIST OF FIGURES

ABSTRACT

A hypothesis by *Maul* [1977], stating the rate of change of Loop Current (LC) volume is related to deep Yucatan Channel (YC) transport, is examined and validated with a continuous 54-year simulation of the regional 1/25˚ Gulf of Mexico (GoM) Hybrid Coordinate Ocean Model (HYCOM). The hypothesis states that the imbalance of transport between the upper YC and the Florida Straits controls the rate of change of the LC volume and that the imbalance is compensated by transport through the deep YC. Previous studies have investigated the relationship between deep YC transport and LC area (used as a proxy for the volume). The first attempt by *Maul et al.* [1985] using a single mooring was unsuccessful in finding a relationship. However, *Bunge et al.* [2002] using data from the Canek observing program, which deployed 8 moorings across the YC, found a strong relationship between the deep YC transport and the LC area. The data used in *Bunge et al*. [2002] was for a period of 7.5 months, which is relatively short compared to the time scale of LC variability. A multi-decadal (54 years) HYCOM simulation of the Gulf of Mexico provides long term data to study LC variability and allows one to validate the *Maul* [1977] theory. Time evolution of the LC between two shedding events can be viewed as a combination of relatively high-frequency (on the order of about 40 days) fluctuations superimposed on a low-frequency trend. The high frequency portions of the modeled variability are shown to be related when the LC-area time derivative and the deep YC transport are compared. The low frequency variability is examined by comparing the LC-area time series with integrated transport in the deep YC, and statistically similar trends are identified. The results support the *Maul* [1977] theory.

CHAPTER ONE

INTRODUCTION

The Loop Current (LC) is a part of the Gulf Stream that enters the Gulf of Mexico (GoM) through the Yucatan Channel (YC), loops in a clockwise manner, and exits through the Florida Straits (FLS). The location and growth rate of the LC are highly variable on an annual time scale. The LC goes through several phases during its life cycle. During a retracted phase, the LC does not extend far into the GoM and it is stable. When extended far north, the LC sheds loop current eddies (LCEs), which are large anticyclonic rings that break off from the LC, referred to as a shedding event, and propagate westward through the GoM. As shown in previous studies [*Hurlburt and Thompson*, 1980; *Sturges et al.*, 1994] the LC needs to evolve into an "unstable configuration" to shed an LCE. Shedding events, like the LC, are variable in time and difficult to predict. Understanding the mechanisms that govern the LC and LCEs is important for predicting their variability.

Knowledge of the LC and LCEs has several practical implications. The strong currents associated with the LCEs affect oil production in the GoM. Oil rigs are basically floating structures that connect to the ocean floor through long pipes. The strong currents from eddies, which can get as high as 3 m/s, can move the oil rigs and require oil production to be suspended. If an oil rig was scheduled to drill and an eddy shuts down the rig, the cost is about $300,000 per day. Also, LCEs and the LC can generate very strong deep currents in the regions of oil and gas development (*Dukhovskoy et al.,* [2009], *Morey and Dukhovskoy* [2013]). Accurate predictions of the LC and LCEs are necessary for planning oil operations in the GoM.

In addition, the deep, warm water associated with LCEs and the LC can cause a hurricane to intensify as its track passes over these features. For example, in 2005 Hurricane Katrina

intensified from category 3 to category 5 as it moved over the LC. After it passed the LC, the hurricane weakened to a category 3 storm before making landfall. Other significant hurricanes that strengthened while passing over the LC include Hurricane Opal in 1995 and Hurricane Ivan in 2004.

Whether the LC evolution can be predicted is an open question. From altimeter data, *Leben et al.,* [2005] found an almost perfect linear relationship between the northern retreat latitude after the LC sheds an eddy and consequent eddy shedding period. *Lugo-Fernandez* [2007] suggested that the LC could be viewed as non-chaotic dynamical system with limited predictability. Nevertheless, LC behavior is irregular and its prediction is still challenging especially in practical applications. A better knowledge of the mechanisms controlling the LC behavior may provide additional insight into limitations and possibilities of LC predictions.

This study investigates the relationship between deep YC transport and LC volume changes. *Maul* [1977] first suggested that the LC grows because of a mass imbalance between the transport into the GoM through the upper YC and the transport out through the FLS. The LC grows when the mass entering the upper YC exceeds the mass exiting the FLS. Since the rate of change of the GoM's volume is negligible, the mass imbalance created must be compensated for somewhere else. *Maul* [1977] suggested that the imbalance is compensated for with deep flows in the lower YC. Thus, the deep YC transport should be highly related to the rate of change of the LC volume. This is possible because the depth of the YC is about twice that of the FLS. *Maul et al.,* [1985] examined this idea using a current meter placed at the bottom center of the YC. They collected three years of data and found no significant relationship between deep flows in the YC and the rate of change of LC size inferred from the area obtained via satellite

measurements. *Maul and Vukovich* [1993] examined volume transport through the FLS and also did not find a significant relation to the LC area rate of change.

Bunge et al., [2002] used a simple box model to illustrate *Maul's* [1977] theory. They investigated data from the Canek observing program, which deployed eight moorings with acoustic doppler current profilers and current meters across the YC from 8 September 1999 to 17 June 2000. They then obtained a 7.5-month record of deep YC transport to be compared to the LC area determined from 3-day averaged satellite thermal (Advanced Very High-Resolution Radiometer -- AVHRR) images. *Bunge et al.,* [2002] found a very strong relationship between LC area and deep YC flows for their time frame. They attributed the lack of a relationship found by *Maul et al.,* [1985] and *Maul and Vukovich* [1993] to insufficient sampling in the YC. The authors suggested that a longer data set was required to further test and validate *Maul's* [1977] theory.

To further investigate the results of *Bunge et al.,* [2002], this study uses data comprising a uniquely long 54-year run of the $1/25^{th}$ degree GoM Hybrid Coordinate Ocean Model (HYCOM; *Chassignet et al.,* [2003], *Dukhovskoy et al.,* [2013 in prep.]). The model is continuously run for three cycles of 18-years forced with NCEP/CFSR atmospheric fields from 1992 to 2009, and forced at the boundaries by climatological fields derived from the $1/12^{th}$ degree North Atlantic HYCOM. This model run provides a long-term data set that is useful to investigate the relationship between changes in LC area and deep YC transport.

The remainder of this paper is organized as follows: chapter 2 explains *Maul's* [1977] theory using the simple box model from *Bunge et al.,* [2002], chapter 3 describes the model and data, chapter 4 describes the YC flow structure in HYCOM, chapter 5 presents the results from

the study on the relationship between deep YC transport and LC area in HYCOM, and chapter 6 summarizes the conclusions.

CHAPTER TWO

CONCEPTUAL MODEL OF THE GoM MASS BALANCE

The GoM mass balance can be illustrated with a simple box model. Assuming incompressibility in the mass conservation law, the equation for the rate of change of volume in the GoM is

$$\frac{dV_{GoM}}{dt} = T_Y + T_F + R + (P - E), \tag{1}$$

where V_{GoM} is the total volume of the GoM, T_Y is the transport through the YC and T_F is the transport through the FLS (T_F is typically out of the GoM and therefore negative), R is river runoff, P is precipitation, and E is evaporation. *Etter et al.,* [1983] showed that R, P, and E are negligible compared to T_Y and T_F. Also, the rate of change of the GoM's volume is negligible compared to the transports through the YC and FLS. This implies that the volume of the GoM is approximately constant. Therefore, the two transport terms, being the two significant terms, balance out, i.e.

$$T_Y + T_F \approx 0. \tag{2}$$

Since the deepest connection to the Atlantic Ocean through the FLS is approximately 730 m (*Bunge et al*., [2002]) and the depth of the YC is approximately 2100 m, it is appropriate to use two layers for the YC. Thus, equation (2) becomes

$$T_Y^u + T_Y^l + T_F \approx 0, \tag{3}$$

where T_Y^u is the transport through the upper YC, and T_Y^l is the transport through the lower YC.

Although the GoM volume remains mostly constant, the LC volume varies. The LC is generally confined to the depths of the FLS and of the upper YC and therefore the imbalance in mass flux between these two regimes should govern the rate of change of LC volume. Thus, it can be said that

$$\frac{dV_{Loop}}{dt} \approx T_Y^u + T_F. \tag{4}$$

One of the caveats associated with this box model is that it does not consider the loss of volume from the LC to the GoM that would occur during a shedding event. During the period analyzed by *Bunge et al.,* [2002] there were no shedding events. However, during the 54 years of model data used in this study, shedding events do occur. To account for the shedding events, only data for deep YC transport and LC area between shedding events are analyzed to test the theory and previous results.

The relation between the LC area and the deep YC transport is readily obtained by combining equations (3) and (4)

$$\frac{dV_{Loop}}{dt} \approx -T_Y^l. \tag{5}$$

Thus, the rate of change of the LC volume should be approximately equal to the negated deep YC transport, which is the theory presented by *Maul* [1977] and *Bunge et al*., [2002].

The schematic in Figure 1 shows the direction of deep YC transport when (a) the LC is growing and (b) the LC is retracting. When the LC is growing deep YC flow is directed out of the GoM as the LC's deep warm water pushes isopycnals downward. In the schematic there are two layers divided by a single isopycnal for simplicity. This isopycnal is forced downward when the LC grows, which forces deep water out of the GoM. The opposite occurs when the LC is retracting.

Maul's [1977] theory is effectively saying that a larger LC's ispoycnals will push down the lower ispoycnals and basically squeeze water out of the GoM. In the two-layer system presented in the box model the only exit for the deep water is the lower YC.

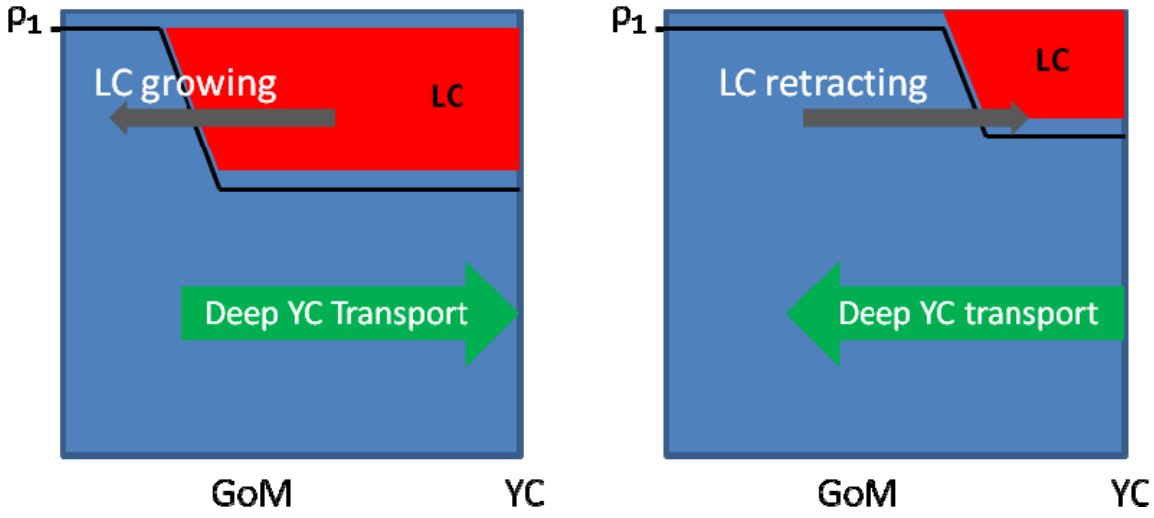

Figure 1. A diagram showing deep water leaving the GoM through the YC when the LC grows and entering the GoM during LC retraction. This is a two-layer system with the upper and lower layer separated by an isopycnal ρ_1.

In previous studies, the deep YC transport was compared to the LC area because the only available observational data of the LC were satellite imagery. Therefore, volume would have to be inferred. Since the LC area is proportional to the volume, this approximation is valid. In this study the LC area is the variable used to maintain consistency with previous studies.

CHAPTER THREE

MODEL AND DATA DESCRIPTION

Data from a 54-year run of the 1/25° resolution regional GoM HYCOM model (*Dukhovskoy et al.,* [2013 in prep]) are used to analyze the relationship between the deep YC transport and the LC area. The domain of the model is 18.9˚N to 31.6˚N and 98˚W to 76.4˚W. Vertically, the model contains 20 hybrid layers. A hybrid coordinate system combines three vertical coordinates; it is isopycnal in the open, stratified ocean and smoothly reverts to a terrain-following coordinate in the shallow coastal regions and to z-level coordinates in the mixed layer or unstratified seas [*Chassignet et al.,* 2003]. The densities are chosen such that the layers are compressed in the upper ocean. The model is forced at the surface with Climate Forecast System Reanalysis (CFSR) atmospheric fields from 1992 to 2009 (*Saha et al.,* [2010]). Since there are only 18 years of atmospheric forcing data, HYCOM is run for 3 cycles of 18 years, and the ends of the surface forcing time series are blended for a smooth transition between cycles. The 54 consecutive years provides a uniquely long data set of oceanographic fields in the GoM.

The regional GoM HYCOM is nested in the 1/12° North Atlantic HYCOM, which covers the domain from 27.9°S to 70°N and from 98°W to 36.2°E. The North Atlantic HYCOM has open boundary conditions derived from a bi-weekly climatology produced by four years (2000–2003] of a free running simulation of the 1/12° Atlantic HYCOM. Even though transports at the boundaries of the GoM HYCOM are prescribed the test of the box model theory is still valid since the conceptual box model is in the interior of the GoM regional HYCOM.

The algorithm for detecting the LC front and calculating the area can be found in *Leben* [2005]. The algorithm uses the 17-cm contour of the demeaned sea surface height field to approximate the core of the LC. Then, the LC area is calculated inside the 17-cm contour. LCE

shedding events can be detected from sudden drops in the LC area time series. The analysis of the timing and frequency of these area drops show that HYCOM realistically portrays LCE shedding events.

During the 54 years of daily output data the LC sheds 64 eddies. The separation periods, the amount of time between two shedding events, help show the robustness of the model. The model is compared to 27 years of observational data from altimeter-based SSH gridded fields. This analysis of the observational data yields a mean separation period of 8 months, a median of 6.4 months, and a mode of 6 months. The HYCOM mean separation period is 10 months, the median is 6.3 months, and the mode is 4 months. Observations have shown a range of separation periods from less than a month to 20 months (*Leben et al.* [2005], *Vukovich* [2007]), whereas HYCOM ranges from 1 to 48 months. The 48-month separation period occurs once, and there are several separation periods over 19 months, indicating that the model can simulate long separation periods that have not observed. However, the mean, median and mode are robust estimators and they are reasonable in the simulation. The histogram shown in figure 2 illustrates the range of separation periods occurring in the model simulation and their frequency of occurrence.

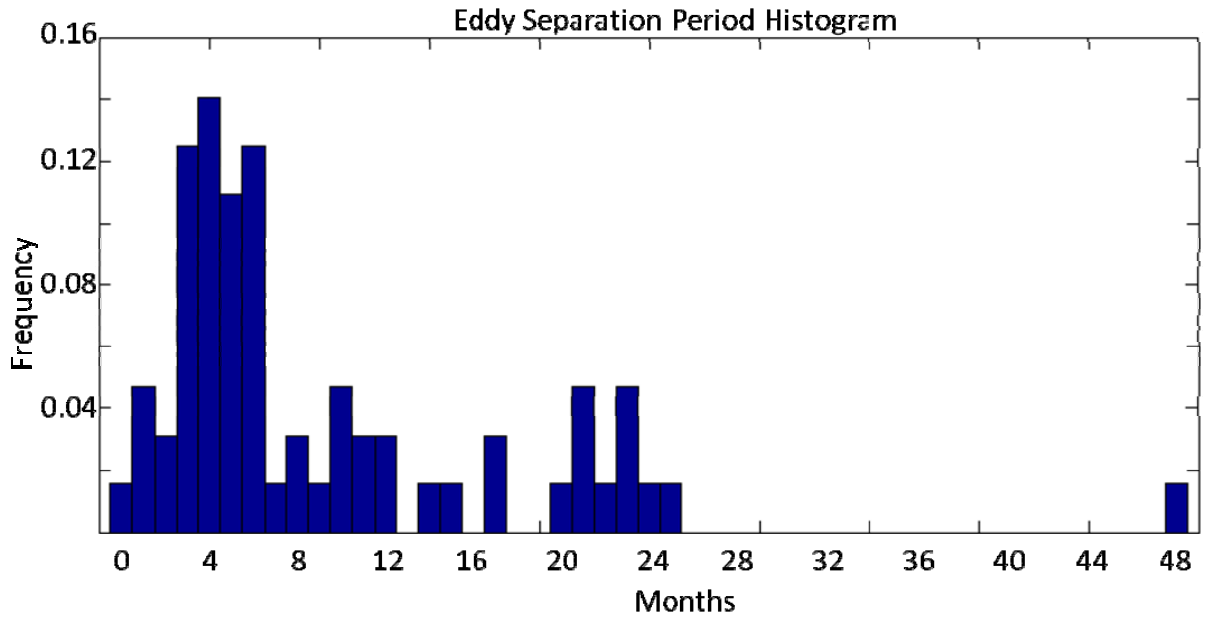

Figure 2. Normalized histogram of the LCE separation period from the 54-year HYCOM simulation. The separation periods on the x-axis are in units of months.

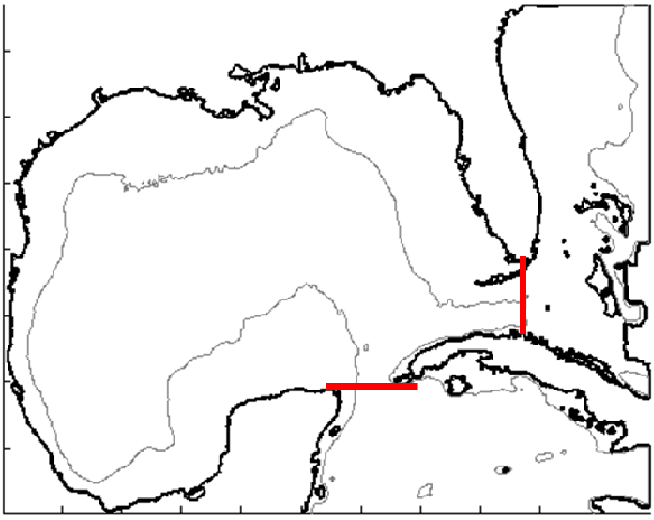

Figure 3. The GoM; red lines indicate locations where the transport was calculated in HYCOM.

According to *Maul* [1977] and *Bunge et al.,* [2002], the LC freely flows from the upper YC to the FLS. Flow that enters the GoM through the deep YC must also exit through the deep YC and therefore the mean flow though the deep YC must be zero, which is seen in the model.

To accurately test the box model theory it is necessary to determine which layers make up the deep YC. These are the vertical layers that have no interaction between the GoM and the Atlantic Ocean through the FLS. Using layer thicknesses, depicted in Figure 4 for the 18th isopycnal**,** it is seen that the 18th isopycnal does not connect the GoM to the Atlantic, implying that the 18th isopycnal and below make up the deep YC. The average transport through the YC for the 18th layer and below is 0 Sv for the long term.

In this study, time series of the daily deep YC and the LC area derived from the 54-year HYCOM run are analyzed. Additionally, the HYCOM transport time series are computed for the entire YC, the upper YC, and the FLS (shown in Figure 3).

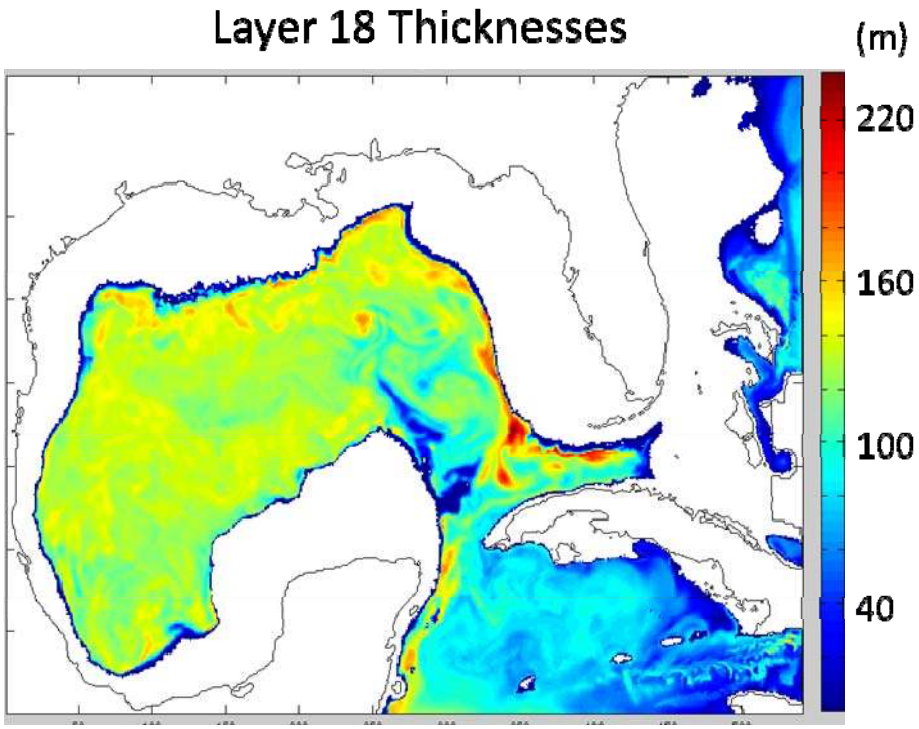

Figure 4. The layer thicknesses for the 18th vertical layer (target density of 1027.64 kg/m^3) in HYCOM. There is no connection along this isopycnal between the GoM and the Atlantic through the FLS.

CHAPTER FOUR

FLOW STRUCTURES AND LC RECIRCULATION

4.1 YC Flow Structure

Before analyzing the transport time series, it is necessary to determine whether HYCOM portrays the YC and FLS accurately. Then, to fully understand the mass imbalance and its causes it is important to understand the variability of the flow structure in the YC and FLS.

The time series of the total HYCOM transports through the YC and FLS (T_Y and T_F) are examined. The two time series are highly related, with a correlation coefficient of .98, and they both have a long-term average of approximately 29.5 Sv. This is larger than estimates obtained from the Canek observing program (*Sheinbaum et al*. [2002]) which yielded a mean transport of 23.1 Sv. However, recent observational data from *Rousset and Beal* [2010] yielded a mean transport of 30.3 Sv over the period of 2001 to 2005. Thus, the mean transport from HYCOM is within the range of recent observational data. The close relationship between the YC and FLS flows is expected because of equation (2) and the relationship implies that equation (3) is also correct.

A 54-year mean vertical structure of the northward velocity through the YC is shown in figure 5a. From this image multiple features are evident. For example, the Yucatan Current, which consists of strong inflow into the GoM, is mainly located in the upper west portion of the YC. Also, there is consistent flow out of the GoM in the upper east portion of the YC. This return flow is referred to as the Cuban Countercurrent (the return flow associated with the Cuban Countercurrent is not part of the mass balance analysis, discussed further below).

The YC should be divided into a western portion of inflow and an eastern portion of return flow. These features vary in time with the size of the LC. The mean structure is consistent

with observational data from the Canek observing program presented by *Sheinbaum et al*., [2002]. Figures 5b-c show the maximum and minimum northward velocities through the YC. A strong Yucatan current and a weak Cuban Countercurrent, features of the maximum YC flow structure, are characteristics of the YC flow structure when the LC is large. When the LC is small the YC flow structure resembles the minimum northward velocity YC flow structure.

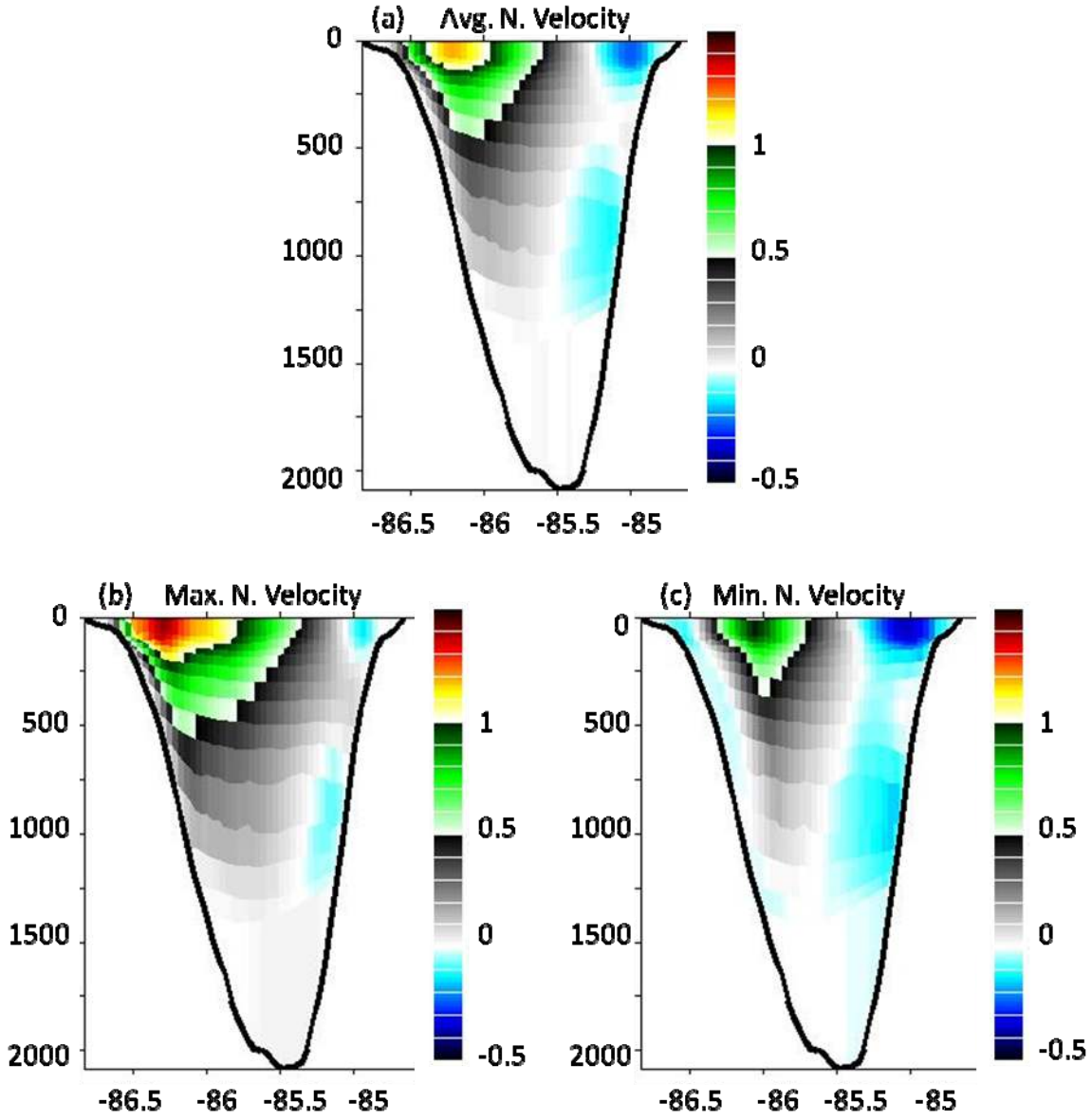

Figure 5. (a) Mean, (b) maximum and (c) minimum northward velocity structures in the YC. The units of the color bar are m/s. The x-axis is longitude and the y-axis is depth (m).

Figure 6a shows the normalized LC area histogram with the 25th and 75th percentiles marked. Figure 6b shows the transport profiles of the upper YC (upper 17 vertical layers) for the LC area greater than the 75th percentile and lower than the 25th percentile, as well as the mean transport profile. Here, transport into the GoM is considered positive. When the LC area is below the 25th percentile (red line), the YC current shifts east and broadens, the maximum transport decreases, and the return flow is weak. When the LC area is larger than its 75th percentile (green line), the YC current shifts west, the maximum transport increases and the return flow out of the GoM increases. This behavior is indicative of a recirculation occurring when the LC is large. When the LC is large and the Yucatan Current is shifted west, there is room for part of the LC to recirculate out through the eastern YC, which yields a strong relationship between the LC and the return flow of the Cuban Countercurrent.

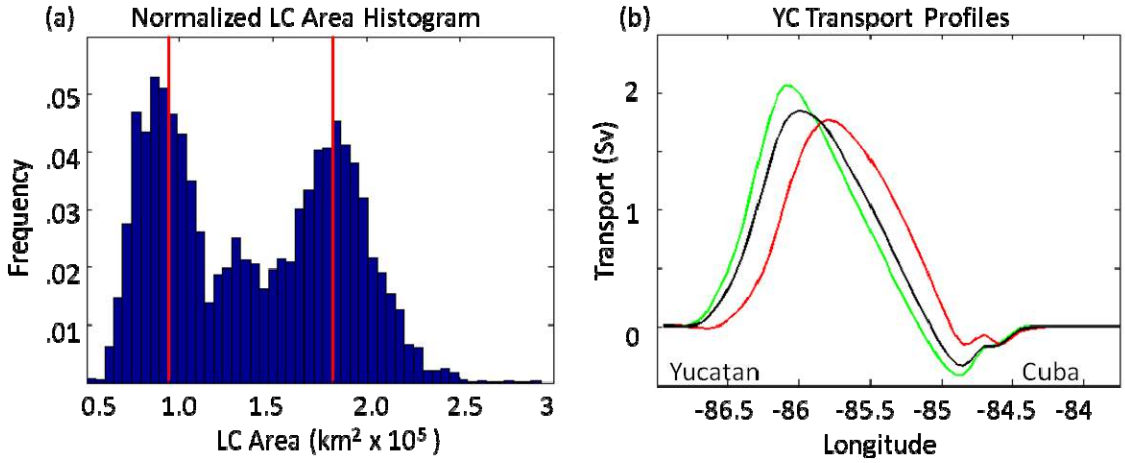

Figure 6. (a) Normalized LC area histogram with red lines representing the 25th and 75th percentiles. (b) Mean transport (Sv) profiles of the YC when the LC area is larger than its 75th percentile (green) and less than its 25th percentile (red). The mean for the entire simulation is shown in black.

The importance of the recirculation lies in the fact it explains why the relationship between the LC and the Cuban Countercurrent is not enough to explain the rate of change of LC

area. Based on the strong relationship between the Cuban Countercurrent and the LC area, one may think the return flow of the Cuban Countercurrent explains the LC growth rate. However, since the Cuban Countercurrent is confined to the upper YC recirculation, it is not enough to explain the mass balance required to keep the GoM volume constant. The reason the mass must be balanced by the deep YC is due to the fact that as the LC grows isopycnal layers are forced deeper in the GoM , and deep water must exit the GoM through the deep YC.

SSH contours (Figure 7) to a first approximation are a good representation of stream functions. Figure 7b shows SSH contours when the LC area is large (i.e., greater than the 75th percentile). Here, some of the contours on the eastern side of the LC show flow returning through the YC, which would enhance the Cuban Countercurrent. Figure 7a shows the SSH contours when the LC area is small (i.e., less than the 25th percentile) and the return flow is much weaker (demonstrated in figure 6b by the transport profile for the 25th percentile and lower LC area).

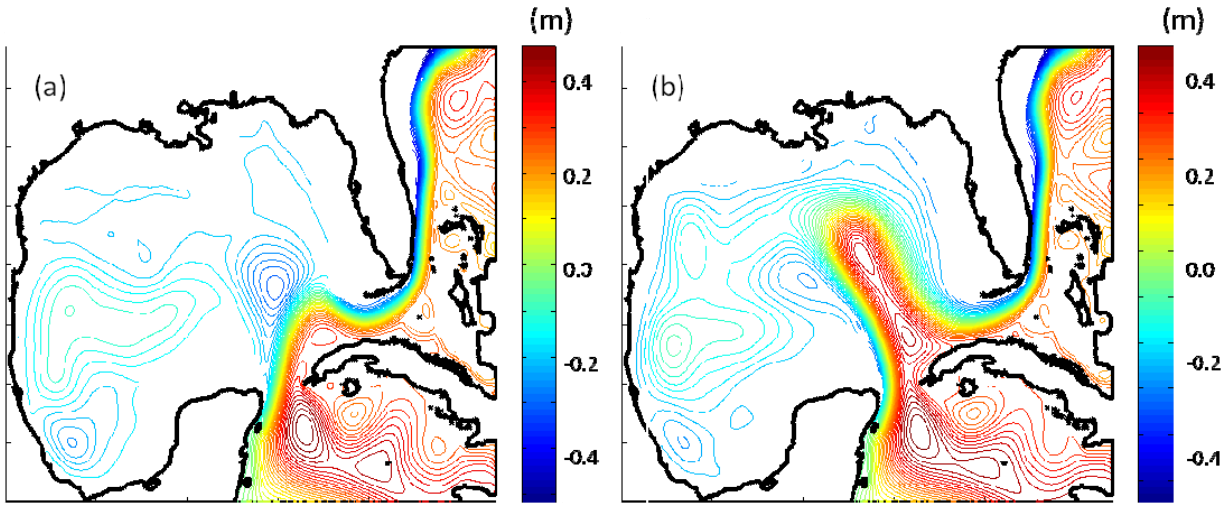

Figure 7. Contoured mean SSH in meters when the LC area is (a) smaller than its 25th percentile (b) larger than its 75th percentile. In both cases recirculation flow appears in the eastern YC due to an anticyclonic pattern west of Cuba.

To further examine the recirculation, the time series of the west YC transport and the LC area are compared. The west YC here is defined as everything west of 90.05°W, the center of the Yucatan Current's mean transport profile peak. When the LC area is large, the current shifts west of this point and narrows, and the maximum transport strengthens; when the LC area is small, the current shifts east of this longitude and broadens, and the maximum transport decreases. The correlation coefficient for the two time series, the LC area and the west YC transport, is .70. The correlation for the negated east YC transport and the LC area is also .70.

Thus, results from the simulation suggest an apparent relationship between the LC and the intensities of the YC current and the Cuban Countercurrent. Therefore, one may think that the return flow seen in the Cuban countercurrent explains the mass balance of the GoM and therefore the LC growth rate. However, this strong correlation between the LC area and Cuban Coutnercurrent is caused by the recirculation. Thus, some fraction of the mass influx does not contribute to LC growth and quickly leaves the GoM as part of the Cuban Countercurrent. This helps explain why this recirculation cannot be used as an indicator of the LC growth rate.

It is useful to think of the upper YC transport in terms of equation (6).

$$T_y^u = T_y^{u+} + T_y^{u-} \tag{6}$$

T_y^{u+} is the flow into the GoM, mainly to the west, through the upper YC and T_y^{u-} is the outflow. T_y^{u+} and $-T_y^{u-}$are well correlated, with a correlation coefficient of .73, as suggested by the recirculation.

Thus, mass leaves the GoM through both the YC (T_y^{u-}) and T_f. For the LC to grow the T_y^{u+}needs to exceed $\mathrm{T_y^{u-}} + T_f$. So, even though the Yucatan Current (mainly T_y^{u+}) may be strong, the LC might not be growing if ($T_y^{u-} + T_f$) is also large. The LC should grow only if there is a mass imbalance, according to *Maul's* [1977] theory. Even though T_y^u consists of a

recirculation, T_y^{u+} and T_y^{u-}, the conceptual model still works. T_y^l still balances the difference between the T_y^u and T_f, as seen in equation (7).

$$\left(T_y^{u+} - T_y^{u-}\right) + T_f \approx T_y^l \tag{7}$$

4.2 FLS Flow Structure

The mean FLS transport profile is directed entirely out of the GoM and therefore it is much simpler than the YC profile. The HYCOM 54-year mean FLS transport profile can be seen in figure 8. There is no evident flow back into the GoM, and the structure of the FLS transport profile is consistent in time. The FLS transport profiles when the LC area is above the 75th percentile and below the 25th percentile both show profiles similar to the mean.

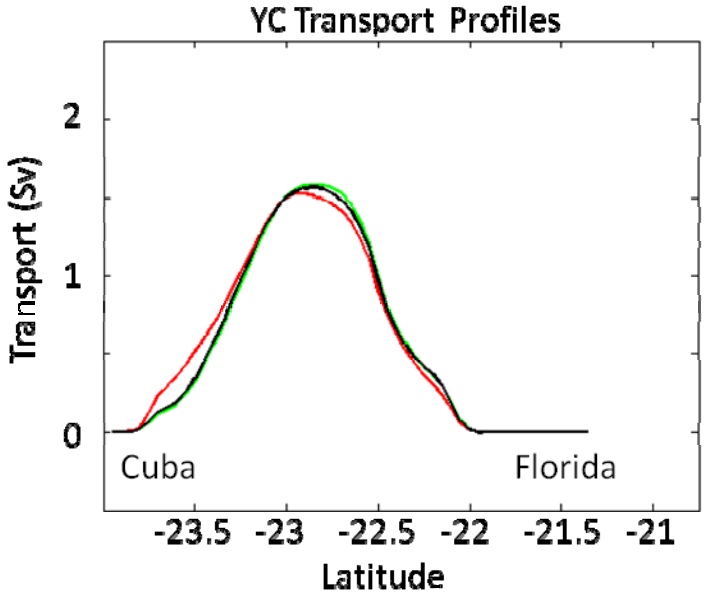

Figure 8: Mean FLS transport profile for the 54 year HYCOM simulation (positive transport is out of the GoM). The transport is directed entirely out of the GoM across the FLS, indicating that there is not a significant counterflow in the FLS, as there is in the YC. Upper 75th percentile and lower 25th percentile transport profiles are shown in green and red respectively.

This suggests that the YC transport fluctuations are balanced by countercurrents in the YC, not the FLS. Since the Cuban Countercurrent is not the balancing flux, deep YC transport must balance the upper YC transport, as suggested by *Maul* [1977] and *Bunge et al.,* [2002].

CHAPTER FIVE

RESULTS OF BOX MODEL THEORY VALIDATION WITH HYCOM

To test the hypothesis presented by *Maul* [1977] and to expand on the results of *Bunge et al*. [2002], two equations from *Bunge et al.* [2002] are analyzed. First, after stating that the LC area is proportional to its volume, equation (5) can be rewritten as

$$H\frac{dA_{Loop}}{dt} \approx -T_y^l, \tag{8}$$

where *H* is a constant scale depth approximating the bottom of the LC and A_{loop} is the LC surface area. The scale depth H was chosen to be 200m. This choice of H yields a nearly one to one ratio between the left and right hand sides of equation (8). Subsequent sections will demonstrate the accuracy of this approximation. This ratio is proportional to H; the time rate of change of the LC area should be related to deep YC transport. If the left hand side of the equation is negative, the LC is retracting. Equation (8) is a relationship of derivatives and therefore represents a high-frequency comparison between the LC-area time derivative and the deep YC transport. Low-frequency variability, examined through integration of equation (8)

$$A_{Loop} = A_0 - \frac{1}{H}\int_{t_0}^{t_f} T_y^l(t)dt, \tag{9}$$

where A_0 is the initial LC area at the initial time t_0, t_f is the final time, and *t* is time.

Bunge et al. [2002] showed that both equations (8) and (9) held true for a period of observational data from the Canek observing program. The time range was 7.5 months, which is too short compared the time scales of LC variability to thoroughly test the box model theory. The data from a 54-year run of HYCOM present an opportunity to investigate the theory for a

much longer period. *Bunge et al*. [2002] investigated the balances given by equations (8) and (9) using correlations; therefore, correlations are used in this study as a subjective analysis tool.

There was no shedding event in the period analyzed by *Bunge et al*. [2002]. Also, the box model theory does not account for shedding events, as explained previously in chapter 2. For the theory to hold throughout time, and include shedding events, another term needs to be included in the equations to account for extreme losses of volume from the LC after a shedding event. Otherwise, this volume would have to be accounted for by very fast transport out through the deep YC, which would be unrealistic. Instead, to test the box model theory, the LC-area time series for HYCOM is segmented into separation periods. A separation period begins the day after a shedding event occurs and ends a day before the next shedding event.

There are 64 shedding events in the HYCOM simulation and therefore 63 separation periods. The distribution of the separation events was discussed in chapter 3 and shown in figure, 2. For this study, only separation periods of 300 days (the mean separation period) or longer are considered to give a better indication of the validity of the hypothesis since testing the theory over longer periods yields a more robust result.

There are 22 separation periods longer than 300 days for analysis. Each time segment begins 30 days after the previous shedding event and ends 30 days before the next shedding event to allow for an adjustment period. The total of the 22 separation periods is 11,722 days, about 32 years of model data for analysis. This amount of time still provides the long period desired to validate the *Maul* [1977] theory.

5.1 High-Frequency Variability Comparison

The high frequency variability between the LC-area time derivative and the deep YC transport can be compared using equation (8). For the high-frequency variability time series the correlation coefficients are negligible without filtering. *Bunge et al.* [2002] discovered that filtering with a 20-day running mean revealed a significant relationship. Thus, for the model data, a 20-day running mean is applied to the LC-area time derivative and the deep YC transport. With the application of the low pass filter, the time series still have high frequencies compared to the time scales of LC variability.

The LC-area time derivative with the filter is calculated using equation (10)

$$\frac{dA_{Loop}}{dt}(i) \approx \frac{\frac{\sum_{i}^{i+\Delta i/2} \bar{A}_i}{\Delta t} - \frac{\sum_{i-\Delta i/2}^{i} \bar{A}_i}{\Delta t}}{\Delta t}. \tag{10}$$

This equation applies a centered difference of the 20-day averages before and after a given day where Δt is the change in time between the center points of the averaged areas, and Δi is the corresponding number of time steps. The variable $\frac{dA_{Loop}}{dt}$ is compared to the 20-day running mean of the deep YC transport from Eq. (9) and calculated using equation (11)

$$T_y^l(i) \approx \left[\sum_{i-\Delta i/2}^{i+\Delta i/2} T_y^l\right]/\Delta t \tag{11}$$

After the low pass filter is applied, a relationship becomes evident in HYCOM data. The correlation coefficient for the overall 20-day smoothed time series is .39. This correlation is not strong, however, as seen in figures 9a-c, which show examples of these time series plotted together, the two series appear to be more closely related than indicated by solely by that correlation.

Analyzing each separation period individually, we generally see that the correlation is quite strong (>.50), however there are some segments where the correlation is weak. Three of

the correlations fall below .10. The main reason for the weak correlations is significant variability in the LC area derivative on short time scales. Variability is attributable to reattachments and quick, small changes in LC area. When a reattachment occurs, the LC-area time derivative first captures the sudden drop, and then captures a sudden peak because of the instant increase in area that follows shortly after. The effect on correlations for a given time series depends on the length of time the eddy is detached, the size of the eddy that detaches, the length of the separation period, and the length of the time series. For example, if, in one of the shorter segments, an eddy detaches from the LC and remains detached for a couple of weeks, the 20-day, smoothed LC-area derivative time series will have a long, steep drop and long, steep rise as seen in Figure 10. If the separation period were quite long, a single reattachment would not have as significant an effect on the correlation.

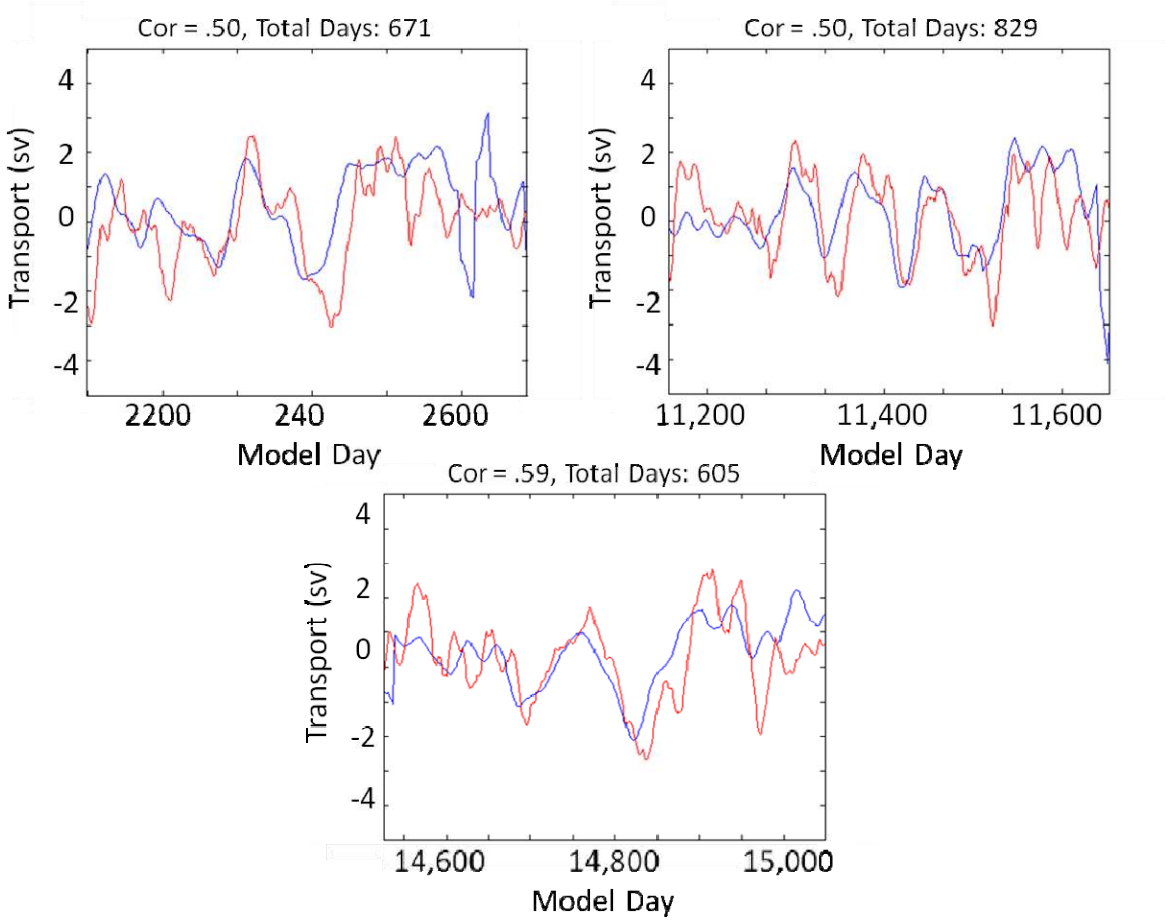

Figure 9. The scale depth *H* multiplied by the LC-area time derivative (blue) and deep YC transport (red) for three separation periods. The correlations and temporal lengths are (a) .50, 671 days, (b) .50, 829 days, and (c) .59, 605 days.

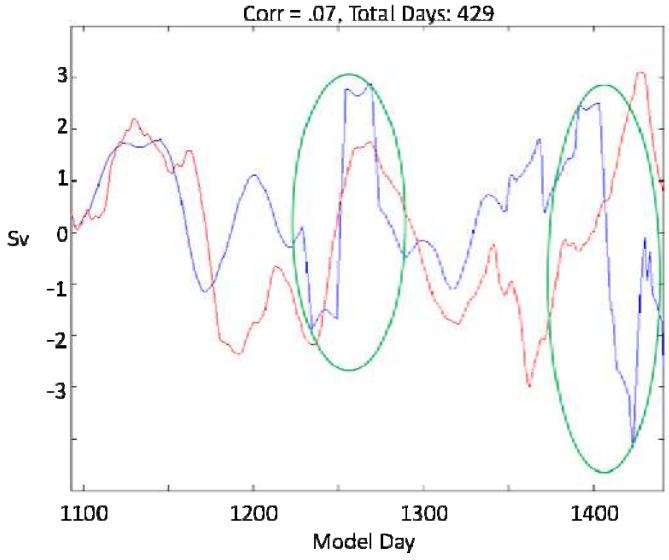

Figure 10. A separation period showing the LC-area time derivative (blue) and the deep YC transport (red). Two eddies detach and subsequently reattach during this period, causing two sudden, large drops followed by sudden large increases (circled in green). The correlation is weak (0.07).

These detachments can be effectively removed by linearly interpolating the LC-area time series, which increases the correlations for the overall time series from .39 to .42. This is not a substantial increase as the LC area derivative is already a highly variable time series. However, several of the shorter separation periods that are heavily impacted by reattachments do increase noticeably. The correlation for the example in Figure 10 increases from .07 to .33.

The correlations are also impacted by an apparent lag in several of the separation periods—the deep YC transport lags the LC-area time derivative. This is very noticeable in Figure 9. *Bunge et al.* [2002] also investigated a lag and found that, for their data, the correlation between the LC-area time derivative and the deep YC transport increased from .62 with no lag to .83 when the deep YC transport lagged the LC-area time derivative by 8.6 days. This was noted as suggestive of an internal adjustment period for the GoM, attributable to the first baroclinic mode of a Kelvin wave. They stated that, using a simple calculation, it was easy to show that the first baroclinic mode of a Kelvin wave would take approximately eight days to travel around the GoM, which is close to this lag time.

For the 22 combined separation periods in HYCOM the correlation is maximized when a lag of 11 days is applied. This lag increases the overall correlation from .39 to .47. This increase seems far less significant than that found by *Bunge et al.* [2002] when a lag is applied. This smaller increase is likely because of the length of the HYCOM series compared to the data from the Canek observing program. The length of the time series and the differences between

the separation periods themselves make it reasonable to apply individual lags to each separation period, thereby providing a distribution of lags, which implies a range of plausible lags.

Figure 11 shows a histogram of the frequency of lags that maximize the correlation for an individual separation period. Six separation periods are ignored here because of their weak correlations. These six periods all have a maximum correlation without a lag. The histogram shows that the majority of the separation periods have a maximum correlation for lags ranging from 9 to 16 days, with 9 days being the most common lag. There are a couple of outliers that yield best lags over 20 days. However, the most frequent best lag, 9 days, is reasonably comparable to that found in *Bunge et al*. [2002] and consistent with an adjustment period related to the first baroclinic mode of a Kelvin wave.

If the two series are filtered for more than the 20 days chosen by *Bunge et al.* [2002], the correlation further increases. A spectral analysis shows there is a peak in the variability of the deep YC transport around 40 days and thus a 40-day filter is applied. *Bunge et al*. [2002] also noted that in their data set there was a dominant mode of variability around 40 days.

The correlation coefficient for the overall time series is .58 when the 40-day filter is used. Therefore, over a third of the total variance is explained. The increase in the correlation is largely due to the decrease in variability of the transport time series. Also, the maximum correlation found with a 40-day smoother increases to .81 from the previous maximum of .70. Then, when the lag of 11 days is applied to the time series with the 40-day running mean, the correlation increases from .58 to .65 and the maximum correlation for an individual separation period is .89.

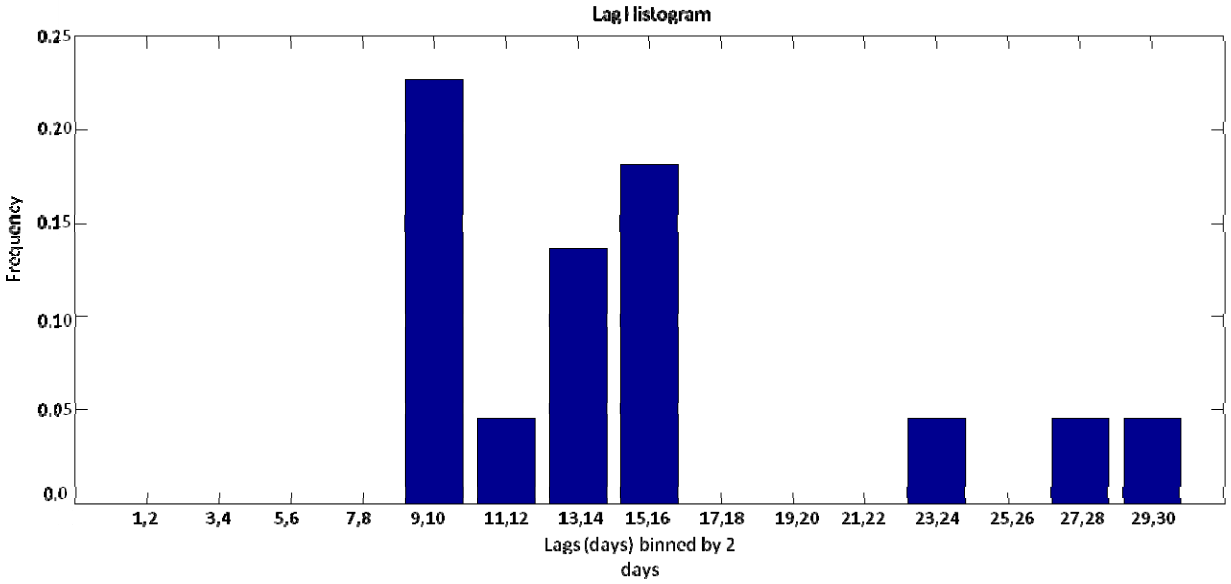

Figure 11. Histogram showing the frequencies at which lags (given in days) maximize the correlation between the LC-area time derivative and the deep YC transport. The lags are binned every two days. The lag that most frequently maximizes the correlation is 9 to 10 days.

The relationship between changes in the LC area and the deep YC transport is further analyzed using a linear regression, and is viewed easily with a scatterplot. Each point on the scatterplot shows the LC-area time derivative for a given deep YC transport. This relationship is not calculated daily because of the strong day-to-day autocorrelation in the LC-area time series. Instead, the LC-area time derivative for the scatterplot is calculated using equation (12)

$$\frac{dA_{Loop}}{dt} = \frac{A_{Loop_{i+\Delta i}} - A_{Loop_i}}{\Delta t} \tag{12}$$

Here, i represents a day in the time series, Δt is the amount of time between two points for which a difference is being calculated, and Δi is the corresponding change in time steps. Thus, equation (12) effectively yields a forward difference over the length of time Δt . Since daily output obscures the relationship in a scatterplot because of autocorrelation, this method, which yields a data point for every number of days Δt, is more efficient. Over the same Δt the deep YC transport is approximated by the average transport.

The scatterplots for the LC-area time derivative versus the deep YC transport initially appear to show some relationship for a majority of the points; however, quite a few outliers, the result of reattachments, obscure the image. Typically, when an eddy detaches the deep YC transport does not react immediately and the LC-area derivative time series quickly dips and spikes. Thus, several points show an excessively large or small LC-area time derivative for a given deep YC transport. Since calculations for the scatter points are not daily, an outlier must be caused when the i^{th} or $(i + \Delta i)^{th}$ day falls on the exact day an eddy is detached. These outliers are removed when the reattachments are removed through linear interpolation.

The scatterplot for Δt =20 days without reattachments is shown in Figure 12. Recall that the LC area time derivative is multiplied by a scale depth H (H= 200m) to yield the same units as transport. The transport is negated here to show a positive slope. It is clear that there is a relationship between the two. The scatterplot is effectively showing that the larger the change in LC area, the stronger the negative deep YC transport. This relationship is the theory presented by *Maul* [1977] and supported by *Bunge et al*. [2002]. The slope for the scatterplot when Δt is 20 days is .9389 Sv. The uncertainty (expressed as a standard deviation) in the slope is .1166 Sv.

The time series of the deep YC transport is found to have a peak in variability around 40 days thus, a scatterplot using a 40-day time change (Δt =40 in equation (12)) is created. Since the time change is doubled, the number of points is then cut in half; however, there are still enough points to show a clear relationship. The slope for the 40-day scatterplot, shown in Figure 13, is 1.0246 Sv, and the uncertainty is .1577 Sv. The scatterplot is an excellent tool as it summarizes all of the separation periods analyzed.

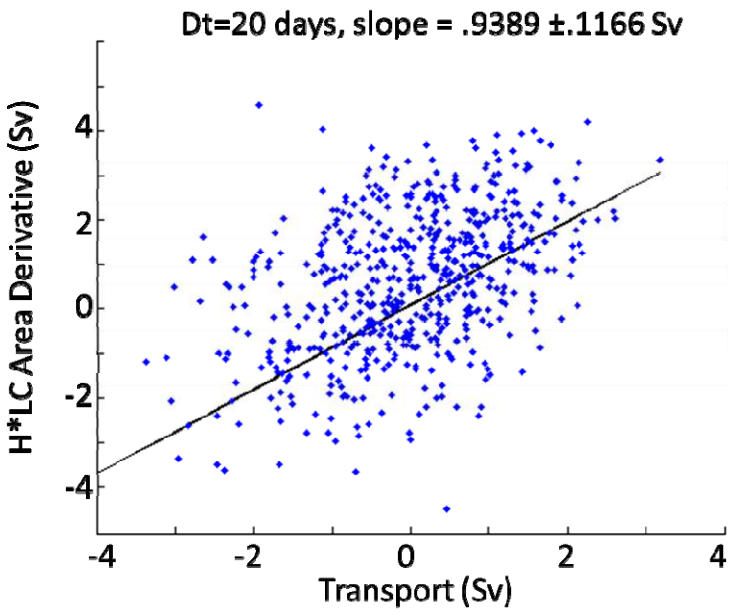

Figure 12. Scatterplot of the LC- area time derivative versus the transport averaged over the same time frame (Δt = 20 days). The slope is .9389 with an uncertainty of .1166 Sv. The LC area is multiplied by a scale depth H for equivalent units.

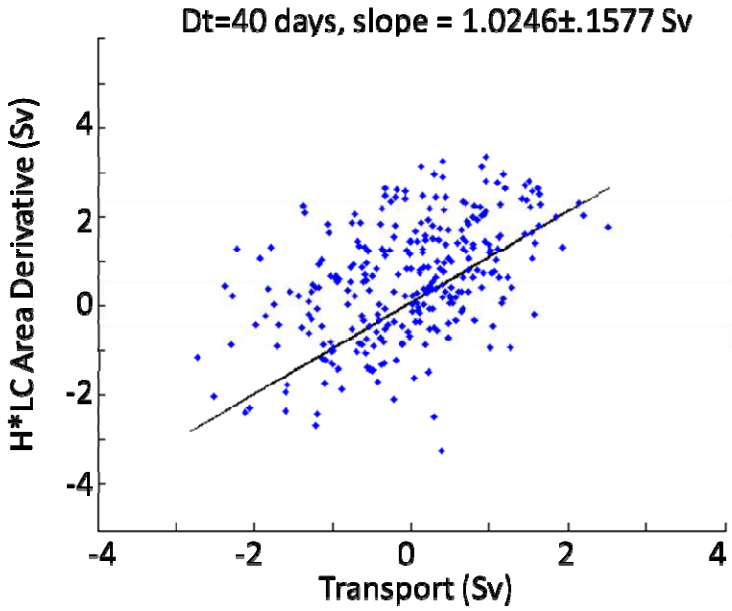

Figure 13. Scatterplot of the LC area time derivative versus the transport averaged for Δt = 40 in equation (10). The slope is 1.0246 with an uncertainty of .1577. The LC area is multiplied by a constant depth H for equivalent units.

The relationship between the LC area time derivative and the deep YC transport is summarized with histograms. The histograms display the frequency at which negative deep transports ($-T_y^l$) occur when the LC-area time derivative is greater than its 75th percentile (Figure 14a), and when the LC-area time derivative is less than its 25th percentile (Figure 14b) for the combined 22 segments. It is clear that for the 75th percentile and above, that $-T_y^l$ is usually positive, that is, out of the GoM (blue in Figure 14). For the smallest area changes (red in Figure 14), which are actually negative, $-T_y^l$ is mostly negative, into the GoM. There is a very clear separation showing that the theory proposed by Maul [1977] is supported in HYCOM. Figure 15 shows the time series of the LC area time derivative with the 25th and 75th percentiles marked. This shows that the 25th percentile LC derivative and below is negative, meaning the LC is retracting. However, the LC is generally growing in the segments analyzed. Since, shedding events are excluded, the LC area derivative is mostly positive as seen in figure 15.

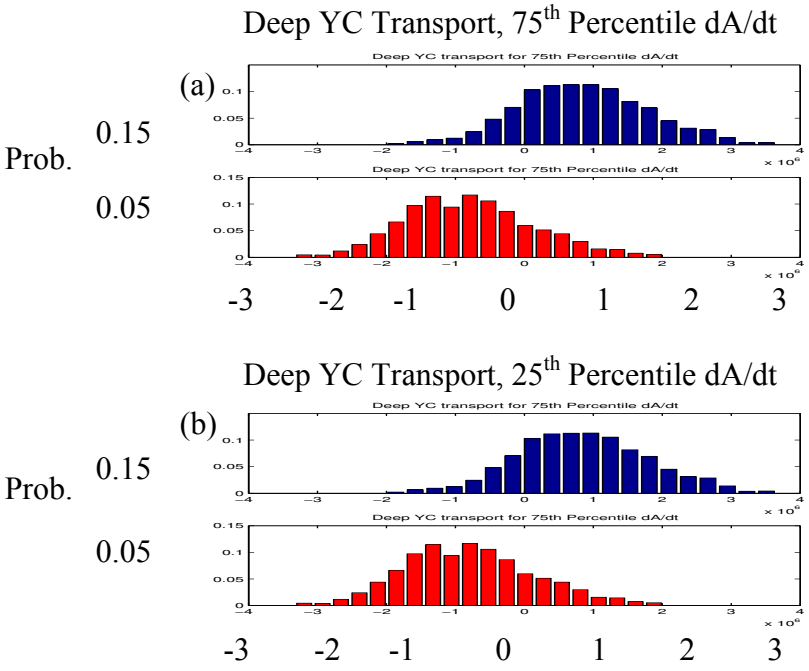

Figure 14: ~~Histograms~~ Probability density function showing the probabilities of negated deep YC transports ($-T_y^l$) occurring when the LC area is (a) greater than its 75th percentile and (b) less than its 25th percentile.

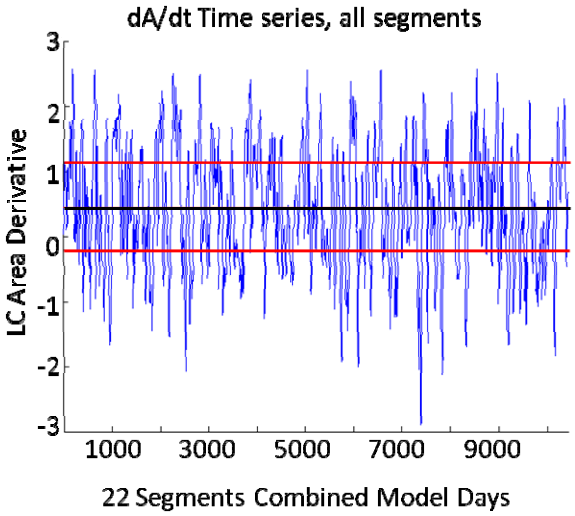

Figure 15. Time series of the LC area derivative multiplied by a scale depth for the combined 22 segments. The mean of .45 Sv is marked by a black line, the 75th percentile of 1.1. Sv and the 25th percentile of -.2 Sv are marked by red lines.

5.2 Low-Frequency Variability Comparison

The time series of the LC area is compared to the time integration of the deep YC transport (9). The time series of the LC area is relatively smooth and changes slowly compared to the transport time series. Therefore, the overall slope of each time series is investigated.

This analysis examines the relationship between the low frequencies of the two time series. It is anticipated that when the LC area increases, the time integration of the deep transport over the same period should increase at a similar rate. This is seen in the model for the time segments analyzed. The overall correlation coefficient between the two time series when all of the segments are combined is .73. Thus, even though the integral of the deep YC transport is much more variable in time than the LC-area time series, the correlation is still high. The correlation between the two series is even higher if the reattachments that occur in many of the segments of the LC-area time series are removed (further discussed below).

When the individual time segments are analyzed, the correlations are often higher than .73; also, several time segments are lower than .73. The worst correlation is .30, and the maximum correlation is .82. The lesser correlations occur mainly because of reattachments. A reattachment occurs when an eddy breaks off from the LC and reattaches after some time. Some eddies reattach after only a day or so, resulting in a sudden drop in the LC-area time series, followed shortly by a sudden jump. In some cases, an eddy may detach from the LC and remain detached for over a week before reattaching. An example of this is shown in Figure 16: there were three reattachments; one eddy detached for 15 days before reattaching. This separation period's correlation of .43 increases to .52 if the separation periods are removed and the LC area is linearly interpolated.

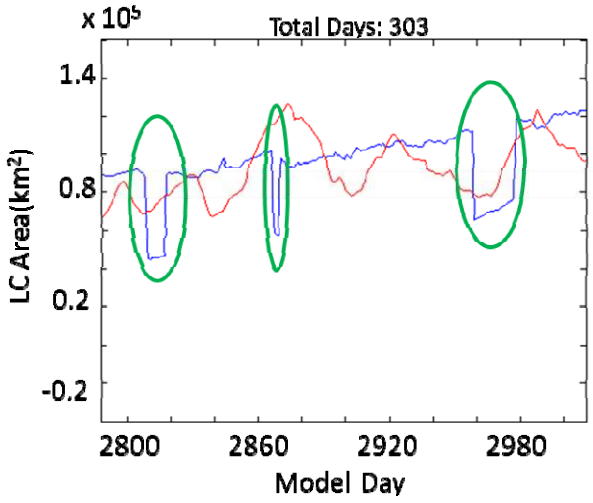

Figure 16. An example of one separation period showing the LC area (blue) and the deep YC transport (red) with reattachments circled in green.

Using the linear interpolation technique to remove brief detachment/reattachment events from the entire time series increases the correlation from .73 to .77. The longer time series are not strongly affected by this technique since the reattachments happen very quickly in

comparison to the length of time. The shorter separation periods are more highly affected but account for less of the overall correlation.

Matching linear regressions are easily seen in Figure 17a-c, which show three examples of separation periods. The consistency of the slopes between the time integrated deep YC transport and LC area supports the conceptual model. The similarities are evident throughout the overall time series as well, but the series is too long to show in a clear figure.

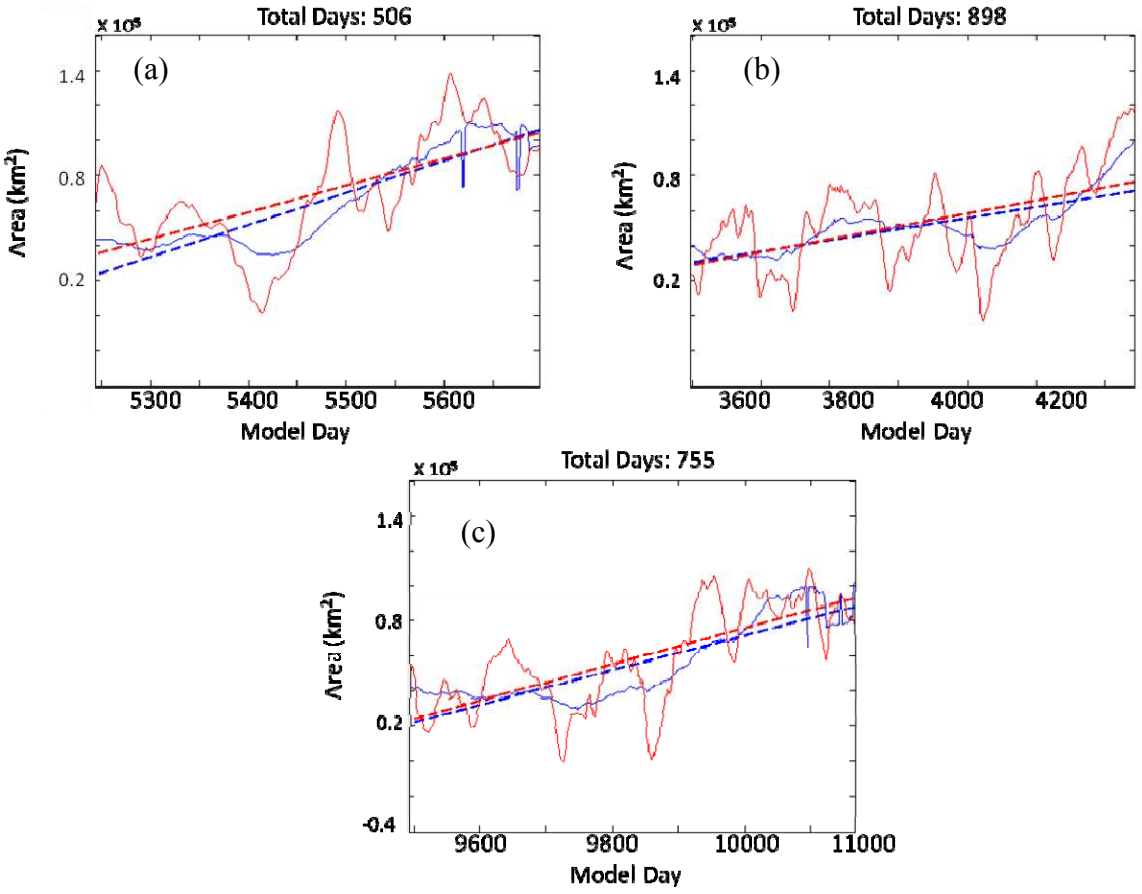

Figure 17. LC area (blue) compared to the time integrated deep YC transport (red) for three separations periods. Trends are shown with dashed lines with respective colors. Their correlations and temporal lengths are (a) .82, 506 days, (b) .81, 898 days, and (c) .80, 755 days. The units on the *y*-axis are square kilometers for the area and the transport.

An analysis of each segment's slope from the linear regression yields the statistical significance of the relationship between the LC area and the time-integrated transport. It is found that the linear regressions of the time series are quite similar for each separation period as seen in the stacked bar plot (figure 18). This stacked bar plot shows that the linear regressions' slopes for each segment a quite similar. This is a robust result considering the variation of slopes from segment to segment. The mean slope for the time integrated deep YC transport is 105 km^2/day and 113 km^2/day for the LC area. A *t*-test shows the means to be statistically equivalent, meaning that it is highly likely that these two time series are related. A scatter plot comparing the slopes of the LC area to the slopes of the time integrated deep YC transport is shown in figure 19 along with the linear regression.

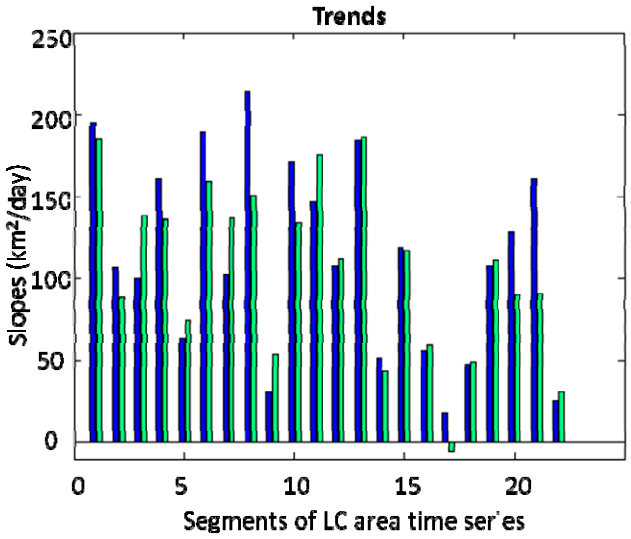

Figure 18. A stacked bar plot of the linear regression slopes for the LC area (blue) and the time-integrated deep YC transport (green) for each separation period.

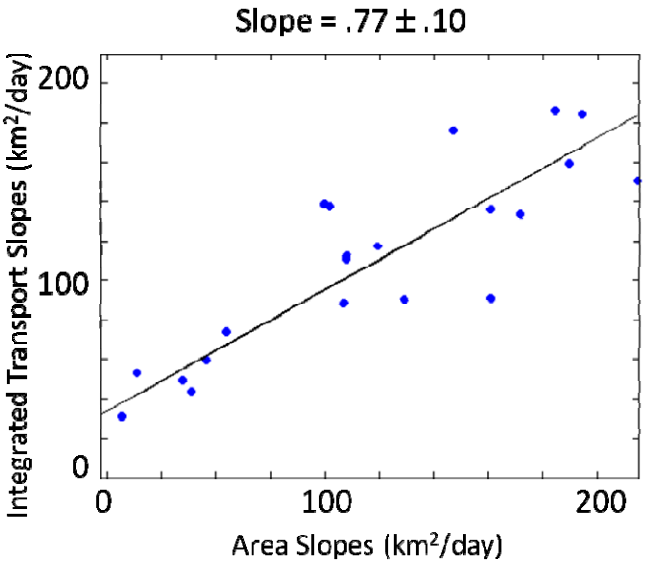

Figure 19. A scatter plot of the LC area linear regression slopes and the time integrated transport slopes.

CHAPTER SIX

CONCLUSION

Data from a 54-year run of the 1/25th degree GoM HYCOM model are used to analyze a theory, first proposed by *Maul* [1977] that changes in LC volume in time should be compensated for by deep flows in the YC. The theory suggests that the change in LC volume is equal to the imbalance between upper YC transport and FLS transport. Since the YC depth (~ 2,000 m) is over twice that of the FLS (~800m), the imbalance is compensated for by deep YC transport.

Bunge et al. [2002] used data from the Canek observing program to show that for the 7.5-month period of data, the deep YC transport was highly correlated to the LC-area time derivative. Only seven months of data were used in *Bunge et al*. [2002], a very short amount of time for testing LC variability; therefore, longer data periods are needed to support the theory. The 54-year run of HYCOM provides a unique data set, because of its length, to test this theory.

Data from the HYCOM simulation are used to calculate transport through the model YC and FLS. It is found that the mean transport through each channel is about 29.5 Sv and that the correlation between the two 54-year transport time series is .98. Further investigation of the YC flow structure in HYCOM yields the presence of an inflow into the GoM through the western YC and outflow through the eastern YC. In HYCOM, when the LC is large, the Yucatan current shifts west, the peak transport increases, and the current narrows. As this happens, the Cuban countercurrent is also strengthened. This relationship indicates that there is likely a return flow occurring when the LC is large, shown to a first approximation to be true using contours of the SSH in HYCOM. When the LC area is in its 75^{th} percentile or higher, several contours illustrate how the LC flows back out through the YC. The return flow is found to be much weaker when the LC area is in its 25^{th} percentile or lower.

The box model theory is tested in HYCOM after the deep YC is defined as the 18^{th} isopycnal (target density of 1027.64 kg/m^3) and below. To accurately test the box model theory it is necessary to use segments between eddy shedding events. Of the 63 available separation periods, 22 are used. The selection criterion is that the separation period has to be at least 300 days (the mean separation period) or longer.

A conceptual model of the GoM mass budget is tested using the 54-year simulation. The first equation tested, equation (8), is used to compare the high frequency relationship between the LC area and deep YC transport. Because of the high frequency variability is large, it is necessary to use a low pass filter to see the trend during separation events. Eeven with the low pass filter the time series is still high frequency compared to LC area variability. After a 20-day running mean for each time series is applied, a relationship between the two time series becomes evident. Though the correlations are fairly weak (for the combined 22 separation periods it is

only .39), it is clear that when the LC is growing, more mass is leaving the GoM through the deep YC and hence there is an imbalance between the upper YC transport and the FLS. Most of the separation periods have obvious relationships whereas 5 of the 22 segments have no apparent relationship. Weak relationships are due to high variability and eddy reattachments; the relationships improve after linearly interpolating for reattachments. When a 40-day running mean is applied, the relationship becomes even clearer, with the correlation for the combined separation periods rising to .58.

For both the 20-day and 40-day running means the correlations are found to increase when a lag is applied to the deep YC transport. The correlation is found to be strongest when the deep YC transport lags the LC area time derivative by 11 days for all of the segments combined. Independently, each separation period has its own best lag. Most frequently, the lags range from 9 to 16 days, which is similar to the 8.6-day lag found in *Bunge et al*. [2002]. The lags can be attributed to a first baroclinic mode Kelvin wave, which takes a little over a week to travel around the GoM.

Scatterplots and histograms illustrate the relationship between the growth of the LC and the deep YC transport. Both the 20-day and 40-day scatterplots show the negated deep YC transport increasing as the LC area growth rate increases. The linear regression shown by the scatterplot illustrates the statistical significance of the relationship. The histogram shows when the LC area is large (greater than the 75^{th} percentile) the deep YC transport is mostly out of the GoM and vice versa when the LC area is small (less than the 25^{th} percentile).

The relationship between the LC area and the time integration of the deep YC transport (equation 9) are tested and used to compare the low-frequency variations in the data. For the 22 separation periods analyzed, there is a strong correlation between the two in HYCOM. The

overall correlation for all of the periods combined is .73. The means of the slopes from the linear regressions of each time series seen in this comparison are statistically equivalent. The low frequency comparison between the LC area and the deep YC transport supports the theory by *Maul* [1977] and the results from *Bunge et al*. [2002].

In conclusion, the theory proposed by *Maul* [1977] and supported by *Bunge et al*. [2002], is further supported by an investigation in the 1/25th degree GoM HYCOM model. Future work using long-term observational data is necessary to conclusively prove the theory.

REFERENCES

Bunge, L., J. Ochoa, A. Badan, J. Candela, and J. Sheinbaum (2002), Deep flows in the Yucatan Channel and their relation to changes in the Loop Current extension, *J. Geophys. Res.,* **107**(C12*), 3233,* doi: 10.1029/2001JC001256.

Chassignet, E.P., L.T. Smith, G.R. Halliwell, and R. Bleck, (2003), North Atlantic simulation with the HYbrid Coordinate Ocean Model (HYCOM): Impact of the vertical coordinate choice, reference density, and thermobaricity. *J. Phys. Oceanogr.,* **33**, 2504-2526.

Dukhovskoy, D. S., Morey, S. L., Martin, P. J., O'Brien, J. J., and Cooper, C. (2009), Application of a vanishing, quasi-sigma, vertical coordinate for simulation of high-speed, deep currents over the Sigsbee Escarpment in the Gulf of Mexico. *Ocean Modelling*, **28**(4), 250-265.

Dukhovskoy D.S., Chassignet E.P., Hall C., Leben R.R., Morey S.L., Nedbor-Gross R. (in prep.) Variability of the Gulf of Mexico Loop Current from a multidecadal simulations and altimeter observations

Etter, P. C. (1983), Heat and freshwater budgets of the Gulf of Mexico, *J. Phys. Oceanogr.*, **13**, 2058–2069.

Hurlburt, H. E., and J. D. Thompson, (1980), A numerical study of Loop Current intrusions and eddy shedding. *J. Phys. Oceanogr.*, **10**, 1611–1651.

Leben, R.R., (2005), Altimeter-derived Loop Current metrics. In: "Circulation in the Gulf of Mexico: Observations and Models", Eds. W. Sturges and A. Lugo-Fernandez, AGU, Washington D.C., doi: 10.1029/161GM15.

Lugo-Fernandez, A., (2007), Is the Loop Current a chaotic oscillator? *JPO*, **37**, 1455-1469.

Maul, G, A. (1977), The annual cycle of the Gulf Loop Current, part I, Observations during a one-year time series, *J. Mar: Res.,* **35**, 29-47, 1977.

Maul, G. A., D. A. Mayer, and S. R. Baig (1985), Comparison between a continuous three-year current meter observation at the sill of the Yucatan Strait, satellite measurements of Gulf Loop Current area, and regional sea level, *J. Geophys. Res.*, **90**, 9089–9096.

Maul, G. A., and F. M. Vukovich (1993), The relationship between variations in the Gulf of Mexico Loop Current and the Straits of Florida volume transport, *J. Phys. Oceanogr.*, **23**, 785–796.

Morey, S. L., and D. S. Dukhovskoy (2013), A Downscaling Method for Simulating Deep Current Interactions with Topography–Application to the Sigsbee Escarpment. *Ocean Modelling*, **69,** 50-63.

Rousset, C., and L.M. Beal (2010), Observations of the Florida and Yucatan Currents from a Caribbean Cruise Ship, *J. Phys. Oceanogr.*, 40, 1575-1581. doi: 10.1175/2010JPO4447.1

Saha, S., and Coauthors (2010), The NCEP Climate Forecast System Reanalysis. *Bull. Amer. Meteor. Soc.*, **91**, 1015–1057. doi: 10.1175/2010BAMS3001.1

Sheinbaum, J., J. Candela, A. Badan, and J. Ochoa, Flow structure and transport in the Yucatan Channel, *Geophys. Res. Lett.*, **29**(3), 1040, doi: 10.1029/2001GL013990, 2002.

Sturges, W., (1994), The frequency of ring separation from the Loop Current in the Gulf of Mexico, J. Mar. Res., **41**, 639-653.

Vukovich, F.M., (2007), Climatology of ocean features in the Gulf of Mexico using satellite remote sensing data. *JPO*, **37**, 689-707, doi: 10.1175/JPO2989.1.

Chang, Y.-L. and L.-Y. Oey, (2013), Loop Current growth and eddy shedding using models andobservations: Numerical process experiments and satellite altimetry data. *J. Phys. Oceanogr.*, **43**, 669-689, DOI: 10.1175/JPO-D-12-0139.1

BIOGRAPHICAL SKETCH

I grew up in Glen Cove, New York and went to college at Johns Hopkins University where I obtained a bachelor's degree in Earth and Planetary Sciences. I took several atmospheric science courses there and realized I had a passion for it and an interest to pursue graduate work in the field. I also took courses in oceanography as an undergrad and enjoyed them as well. This helped me become a researcher at COAPS where oceanography and meteorology go hand in hand.

In addition to my studies at Johns Hopkins I was also a 4-year member of the varsity NCAA wrestling team. Continuing athletics in Tallahassee I play rugby for the Tallahassee Conquistadors.

I am beginning a PhD program at the University of Florida this fall where I will be researching in the air resources department.